ELSEVIER

Polymer 42 (2001) 7943–7952

polymer

www.elsevier.nl/locate/polymer

Quantitative magnetic resonance imaging study of water uptake by polyamide 4,6

P. Adriaensens[a], A. Pollaris[a], R. Carleer[a], D. Vanderzande[a], J. Gelan[a,*], V.M. Litvinov[b], J. Tijssen[b]

[a]*Department of SBG, Institute for Material Research (IMO), Limburg University, Universitaire Campus, Building D, B-3590 Diepenbeek, Belgium*
[b]*DSM Research, P.O. Box 18, 6160 MD Geleen, The Netherlands*

Received 24 January 2001; received in revised form 12 April 2001; accepted 27 April 2001

Abstract

Magnetic resonance imaging (MRI) and NMR relaxation experiments are used to study the water absorption by polyamide 4,6 (PA46) plates. Despite the higher crystallinity, PA46 absorbs more water as compared to the polyamides 6 and 6,6 (PA6 and PA66). Relaxation measurements demonstrate that the volume averaged molecular mobility (T_2^H) of the absorbed water molecules in PA46 is higher than in PA6 and PA66. Quantitative relaxation results of water saturated PA46 further suggest fast exchange between free water and water molecules bound via hydrogen bonds to amide groups. MRI reveals a gradual decrease in the amount and the T_2^H relaxation behaviour of water from the surface towards the core part of PA46 plates. This can be explained by the very high crystallisation rate of PA46, which prevents the close coupling of amide groups in the amorphous phase and results in a larger mean distance between the amide groups, especially in the outer part of the PA46 plates. Density measurements (WAXS and gradient column) show an increase of the density of the amorphous phase during annealing, resulting in a lower water uptake and a lower mobility of the absorbed water molecules.

Keywords: Magnetic resonance imaging; NMR; Relaxation experiments

1. Introduction

In the last decade, a new engineering plastic, polyamide 4,6 (PA46) has been introduced. Because of the high concentration of amide groups, the uniform length of the hydrocarbon segments between the amide groups and the flexibility of the polymer chain, PA46 has a higher melting temperature, a higher crystallinity and a higher rate of crystallisation than polyamide 6 and 6,6 (PA6 and PA66) (Table 1) [1]. Therefore PA46 is easily processed (low cycle-times during injection moulding) and has excellent properties particularly at high temperatures: high stiffness, good toughness, high creep resistance, high fatigue resistance, high resistance against peak temperatures and high thermal stability. PA46 bridges the gap between conventional engineering plastics such as PA6, PA66 and polyesters, and exotic materials such as LCP, polysulfones and PEEK.

Polyamides have the longest history among many synthetic semi-crystalline polymers and are an important polymer material that is used in considerable amounts in the form of fibres, films and plastic mouldings. Polyamides, however, absorb water because of the amide functionality [2]. The absorption of water results in a dimensional change and a lowering of the glass transition temperature (T_g). The higher the level of water absorption, the larger the dimensional change and the drop of T_g. A water absorption of 12.4% in PA46 results in a drop of T_g from 80 down to −40°C. When T_g drops below room temperature, being the usual test temperature, the PAs show lower stiffness, higher toughness and lower electrical resistivity [3,4] since the amorphous phase has been softened by the plasticising effect of the absorbed water molecules.

Despite the higher concentration of amide groups in PA46, a smaller amount of water absorption was expected for PA46 as compared to PA6 and PA66 if the higher crystallinity of PA46 is taken into account (water is only absorbed by the amorphous phase) [5–12]. Surprisingly, PA46 absorbs more water than PA6 and PA66. The aim of this NMR study is to obtain more information about the mechanism of water sorption by PA46.

Gravimetric and radioactive tracer techniques are most commonly used to study liquid transport in polymers [13,14]. While radioactive tracer studies usually require

* Corresponding author. Tel.: +32-11-26-8388; fax: +32-11-26-8301.
E-mail address: jan.gelan@luc.ac.be (J. Gelan).

0032-3861/01/$ - see front matter
PII: S0032-3861(01)00314-7

Table 1
Characteristics of PA46, PA66 and PA6 [1]

	PA46	PA66	PA6
Structure	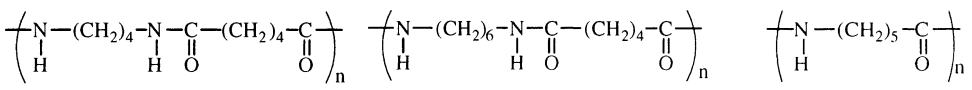		
Crystallinity[a] (%)	60–70	50	50
% water uptake[b]	12.4	8.5	9.5
T_g (°C)	80	65	60
T_c (°C)	260	230	180
T_m (°C)	290	265	220
Crystallisation rate at 200°C/min[c]	>15	6	0.2

[a] % crystallinity determined by WAXS.
[b] Mass percentage of the water uptake by injection moulded plates at 35°C.
[c] Obtained from DSC. From cooling curves at different scanning speeds the correlation between crystallisation rate (= reciprocal time period at half of the maximal height in the crystallisation curve) and crystallisation temperature can be determined.

destructive sample sectioning, a gravimetric analysis is unable to reveal the nature of the fluid absorption profiles and thus relies on a model for the diffusion process. To characterise the water ingress and its effect on structural and dynamic properties in PA46, there is a need for spatially resolved information. Nuclear magnetic resonance imaging (MRI) is a branch of NMR spectroscopy that was first proposed by Lauterbur [15]. It is a unique, non-invasive and non-destructive tool for examining the spatially resolved distribution of the concentration and the molecular mobility of ingressed penetrants. The viability of MRI to investigate mass transport processes in materials has recently been demonstrated [16–26].

In this paper, the combination of gravimetric analysis, DSC, MRI and NMR relaxation is used to study the water ingress into PA46.

2. Experimental

2.1. Materials

Injection moulded PA46 plates (80 × 80 × 2 mm and 80 × 80 × 4 mm) were prepared with a melt and mould temperature of, respectively, 315 and 120°C. PA66 plates (80 × 80 × 2 mm) were melted and moulded at, respectively, 290 and 80°C.

Plates used for MRI (30 × 10 × 2 mm) and for the gravimetric analysis (30 × 10 × 2 mm and 30 × 10 × 4 mm) were sawn out of the original plates. Annealing of PA46 plates was accomplished at 260°C for 12.5 h under N_2-atmosphere. Polished 2 mm plates were obtained by removing 1 mm from both sides of an original 4 mm plate (two-sided polished) or 2 mm on one side (one-side polished) by polishing with emery paper P4000 with a grain size of 4–5 μm.

Proton CPMG T_2 NMR relaxation experiments were performed on small strips of PA46 (30 × 4 × 2 mm) fixed into a standard 5 mm NMR tube. For proton solid echo wide-line NMR relaxation experiments, small pieces of the core part and outer layer (100 and 350 μm) of dry PA46 were packed in a short 5 mm glass tube closed with Teflon stoppers. Deuterium quadrupolar echo spectra were acquired using small pieces of D_2O saturated PA46. These pieces were rinsed with water and dried of excess of water to remove all surface adsorbed D_2O.

2.2. DSC

The melting enthalpy (ΔH_m) and melting point (T_m) of PA46 were measured on a Perkin–Elmer 7, provided with a thermal analysis controller TAC/DX at a heating rate of 10°C/min under nitrogen atmosphere.

2.3. WAXS and density measurements

WAXS (wide-angle X-ray scattering) diffractograms were recorded using a Philips PW 1820 diffractometer system to determine the level of crystallinity and the density of the crystalline phase (ρ_c). The overall densities were determined by means of a density gradient column.

2.4. Gravimetric analysis

The PA46 plates were dried at 100°C for about 14 h to constant weight, M_0. The plates were immersed in distilled water, removed periodically, dried of excess of water and weighed (M_t). The water uptake (in wt%) was calculated according to Eq. (1):

$$\%\ \text{water uptake} = \frac{M_t - M_0}{M_0} \times 100 \quad (1)$$

The rate of water uptake was determined using the

following equation [27–29]:

$$\frac{M_t}{M_{eq}} = \frac{4}{\sqrt{\pi}}\left(\frac{Xt}{l^2}\right)^{1/2} \quad (2)$$

where M_t and M_{eq} are the weight at time t and at equilibrium, respectively, l is the thickness of the plate and X is the rate of water uptake.

2.5. Imaging

MRI images were acquired at 9.4 T on an Inova 400 Varian vertical bore spectrometer using a 16 mm micro-imaging coil with a spin-warp pulse sequence. A dedicated Teflon holder was used to immobilise the plate (30 mm dimension along B_0, Fig. 1).

Standard images of water saturated PA46 plates were obtained with a spin echo time (T_E) of 7 ms and a repetition time (T_R) of 3.5 s. The images have an in-plane pixel resolution of about 60 × 60 mm, a field of view (FOV) of 16 × 16 mm and a slice thickness of 6 mm. Only the central part of the images is used to reconstruct one-dimensional (1-D) projections (cf. below: the area between the two lines A and B as shown in Fig. 2(a)). Images of specimen that were measured as a function of time were acquired in the presence of surrounding water to prevent long term water desorption. The signal from the surrounding water was suppressed by the inversion recovery (IR) technique that is based on the difference in T_1 (the proton spin–lattice relaxation time) between surrounding and ingressed water.

Spatially resolved relaxation and concentration values were obtained by acquiring images of a saturated PA46 plate without surrounding water as a function of T_E and T_R with a FOV of 15 × 5 mm. For the T_E series, T_R was fixed to 3.5 s while T_E was varied between 1.7 and 11 ms in steps of 0.5 ms. For the T_R series, T_E was fixed to 1.7 ms and T_R was varied between 0.05 and 5 s (21 values). The spatially

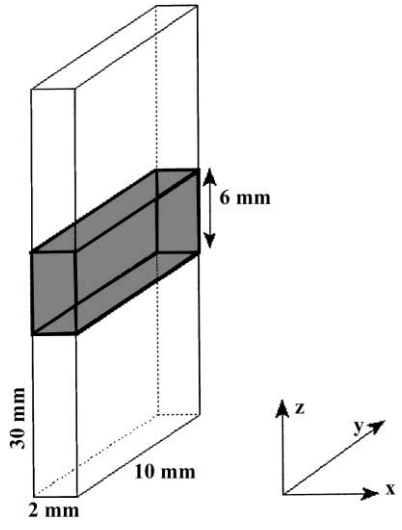

Fig. 1. Size and position of the PA46 plate with respect to the B_0-field (z-direction) of the magnet.

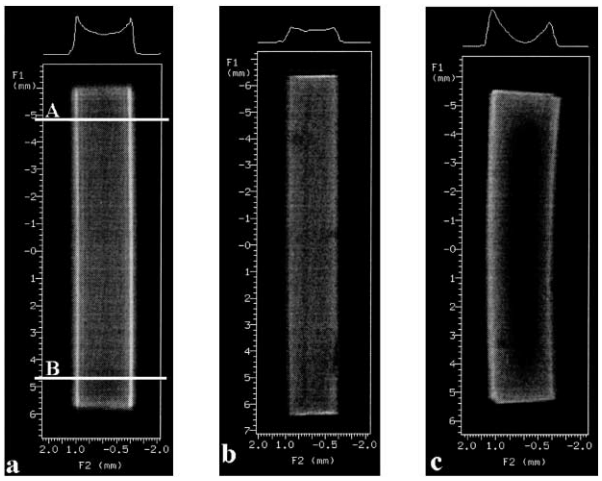

Fig. 2. MRI images of: (a) a saturated PA46 plate (T_E = 7 ms, T_R = 3.5 s) with an indication of the area between the lines A and B, which is used to reconstruct the 1-D projections; (b) a saturated two-sided polished PA46 plate (T_E = 7 ms, T_R = 3.5 s); (c) a partially saturated one side polished (right side) PA46 plate (T_E = 7 ms, T_R = 3.5 s).

resolved values of M_0 (spin density), T_2 (the proton spin–spin relaxation time) and T_1 were calculated from reconstructed 1-D projections (central part between the lines A and B) for consecutive slices of 0.2 mm from the core towards the outer part of the plate by fitting the signal intensity as a function of T_E and T_R, using the following relations [30]:

$$M = M_0 e^{(-T_E/T_2)} \quad (3)$$

$$M = M_0(1 - e^{(-T_R/T_1)})e^{(-T_E/T_2)} \quad (4)$$

Intensity calibrated MRI images were obtained on saturated plates without surrounding water and were calibrated by means of a reference capillary filled with a 0.2% $CuCl_2$ solution in H_2O/D_2O 1/8 (pH = 4.5). The mixture H_2O/D_2O is used to avoid too large differences in dynamic range between the signal of the saturated plates and of the capillary. The T_1 of this reference solution is 0.1 s. Images were recorded with $T_R = 5 \times T_1$ and T_E = 1.25 ms and 5 ms. 1-D projections were reconstructed from the central part of the images. Volume averaged T_1 and T_2 decay times were determined for the same specimen from direct MRI projections (not reconstructed from images) as a function of T_R and T_E. For the T_R series, T_E = 1.25 ms and T_R was varied between 0.1 and 7.5 s. For the T_E series, $T_R = 5 \times T_1$ and T_E was varied between 1.25 and 7 ms.

The quantitative determination of the amount of absorbed water in saturated PA46 was accomplished by acquiring MRI projections (6 mm slice thickness) of a set-up of a water saturated plate and a 5 mm NMR tube (4.2 mm internal diameter) filled with doped (0.2% $CuCl_2$) water as a function of T_E with T_R = 5 s. T_E was varied between 3 and 300 ms (between 3 and 10 ms in steps of 0.25 ms,

between 10 and 20 ms in steps of 1 ms and between 20 and 300 ms in steps of 10 ms.

2.6. Volume averaged NMR spectroscopic relaxation experiments

To record the proton transverse magnetisation decay time of semi-rigid and mobile molecules (like plasticised polyamide and ingressed water), T_2 relaxation experiments were performed on the same spectrometer using a 5 mm dedicated proton probe and the CPMG pulse sequence (Carr Purcell Meiboom Gill) [31]. The spectral width is 200 kHz (5 μs dwell time). Each evolution time of the array is given by the relation: $2 \times n \times \tau/2$, with $\tau/2 =$ 0.1 ms and n an even integer to minimise the effect of imperfections of the 180° refocusing pulses. The protons from rigid molecules (like those of the crystalline and rigid amorphous phase), having a T_2 of about 15 μs are, however, not detected in this experiment.

Proton solid echo wide-line NMR was used to measure the short T_2 decay times of rigid molecules in dry PA46. Since this experiment does not eliminate the effect of magnetic field inhomogeneities, it cannot be used to determine the T_2 relaxation time of semi-rigid and mobile molecules. Solid echo proton spectra were recorded with a dedicated wide-line probe using the solid echo pulse sequence [32] with an echo delay of 8 μs and a 90° pulse width of 1.8 μs. Spectra were recorded with a spectral width of 2 MHz (0.5 μs dwell time) allowing an accurate determination of the echo maximum. The T_2 values were determined by curve fitting of the FID to an Abragam function [33] at room temperature and to the sum of a Gaussian and exponential function [33] at 170°C. The ^{1}H T_1 relaxation times were measured using the inversion recovery solid echo sequence [34].

Deuterium wide-line spectra of D_2O saturated polyamides were recorded by means of the quadrupolar echo pulse sequence with a spectral width of 2 or 40 kHz and a 90° pulse width of 2.4 μs. Deuterium T_1 relaxation times were determined by the inversion recovery method.

All non-linear least-square analyses of relaxation data were performed on a Macintosh computer using the program KaleidaGraph 3.0.

3. Results and discussion

3.1. Gravimetric analysis

Fig. 3 shows the water uptake against the square root of time for a 2 mm plate immersed in water at 35 and 45°C and for a 4 mm plate at 35°C. Although the initial water uptake increases linearly versus square root of time, being indicative for Fickian diffusion [12,29], we prefer to use the term 'rate of water sorption' rather than 'diffusion coefficient' because the morphology of the amorphous phase is not homogeneous over the total cross-section of the plate as will be demonstrated later. For all specimens studied, the water uptake levels off at about 12.4% regardless of temperature and sample thickness.

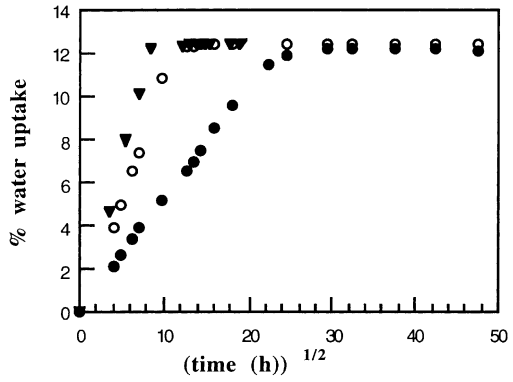

Fig. 3. Water uptake (in wt%) by PA46 plates as a function of square root of time for a 2 mm plate immersed in distilled water at (○) 35 and (▼) 45°C and (●) for a 4 mm plate at 35°C.

The rate of water sorption decreases with decreasing temperature and is slower in a 95% relative humidity atmosphere (results not shown) as compared to that for a sample immersed in water. The rate of water uptake (Eq. (2)) is 1.5×10^{-6} mm^2/s and 2.7×10^{-6} mm^2/s for the water ingress in PA46 plates at, respectively, 35 and 45°C.

3.2. Determination of the volume averaged T_2 relaxation of water molecules in water saturated PA46

In order to have a good estimate of the T_2 decay times of mobile and semi-rigid molecules like absorbed water and plasticised polyamide, a CPMG experiment was performed on water saturated PA46 at 20°C. This temperature is 60°C above the T_g of water saturated PA46 ($T_g = -40$°C). A biexponential analysis resulted in a long T_2 decay time of 4 ms (T_2^l) and a short one of 1.1 ms (T_2^s). A similar T_2 measurement on dry PA46 at 140°C, being also 60°C above the glass transition temperature of dry PA46 (Table 1), resulted in only the short T_2 decay time. These experiments allow us to assign the long T_2 decay time to absorbed water and the short decay time to plasticised polyamide chains in amorphous domains. Since CPMG possibly does not detect strongly bounded water molecules, these experiments do not allow to conclude that all absorbed water is represented by the decay time T_2^l, which would suggest fast exchange between free and bound water molecules.

3.3. Quantitative determination of water in saturated PA46 plates

A straightforward method to judge if all water molecules are represented by the single decay time T_2^l is to compare the amount of water determined by weighing with this derived from slice selective MRI projections in the presence of an internal standard. This was accomplished by acquiring projections of a set-up of a water saturated PA46 plate and a 5 mm NMR tube filled with doped water as a function

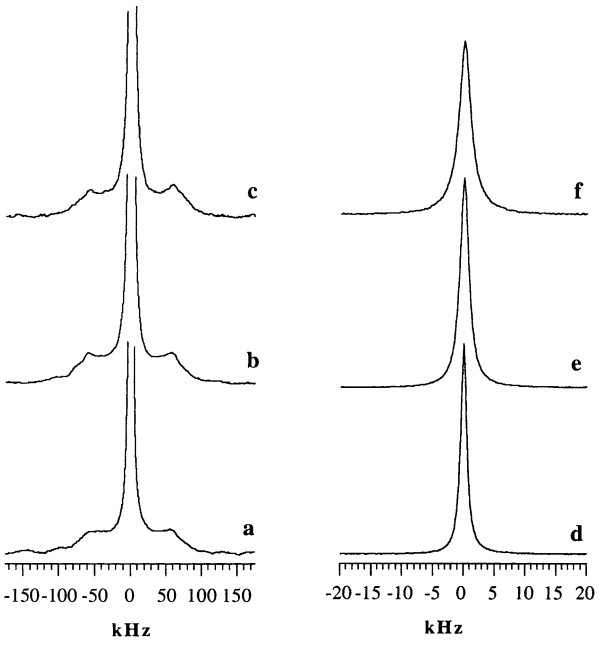

Fig. 4. Deuterium quadrupolar echo spectra, recorded with a spectral width of 2 MHz, of D_2O saturated PA46 (a); PA66 (b) and annealed PA46 (c). Deuterium quadrupolar echo spectra, recorded with a spectral width of 40 kHz, of D_2O saturated PA46 (d); PA66 (e) and annealed PA46 (f).

of the echo time. The quantitative signal intensities (spin densities, M_0) were obtained by extrapolating the projection intensities of both the plate and the tube to $T_E = 0$ by means of Eq. (3). To avoid any contribution of plasticised PA46 to the spin density of water in the plate, only echo time intensities starting from $T_E = 6$ ms were analysed for the plate. These in contrast to the tube, for which echo time intensities starting from 3 ms were used. The spin density of water in the plate was then transformed to mass units on the basis of the known mass (volume) of water in the slice of the tube. Extrapolating to the total height of the plate resulted in the quantitative amount of water in the plate, which is equal to the amount derived by weighing. Reproducible results were obtained in a duplo experiment. This method, which is general applicable, proves that fast local exchange takes place between free and bound water molecules and that all water molecules are represented by a single volume averaged T_2 decay time of 4 ms.

3.4. Volume averaged deuterium relaxation experiments

Fast local exchange of water molecules is further confirmed by solid-state deuterium NMR, a successful technique to study the segmental dynamics of polyamides [35,36]. A deuterium quadrupolar echo spectrum of PA46 saturated with D_2O is shown in Fig. 4(a). The spectrum consists of a narrow line, superimposed on a broad Pake pattern. In agreement with Loo et al. [37], the broad Pake pattern, arising from ND moieties, which are formed by exchange of NH-groups with D_2O in the amorphous phase, only appears in quadrupolar echo wide-line spectra acquired with a short dwell time. The ratio of the integral intensity of the narrow line to Pake pattern is 4.4 to 1. This means that the narrow line represents all water. Indeed, a D_2O mass uptake of 13.7% and an amorphous PA46 content of 30% should give a molar ratio D_2O to ND of 2.2 to 1 (two mole ND-moieties per mole repetition unit of PA46) or a deuterium integral intensity ratio of 4.4 to 1.

Hutchison et al. [7] performed deuterium NMR studies on PA6 fibres saturated with D_2O. By using a spectral width of 40 kHz, which only selects the semi-rigid and mobile molecules, they did discriminate between a narrow line with a long deuterium T_1 value of 200 ms and a signal showing a remaining quadrupolar splitting of about 3.5 kHz with a short deuterium T_1 value of 3 ms. They assigned both signals to loosely and strongly bound water molecules, respectively. Fig. 4(d) shows a quadrupolar echo spectrum of PA46 saturated with D_2O, also recorded with a spectral width of 40 kHz. However, no signal showing a remaining quadrupolar splitting is observed. Only the motionally narrowed D_2O line is observed. A T_1 inversion recovery experiment resulted in just a single deuterium T_1 value of 5.5 ms. No indication for multiple relaxation is observed in the inversion recovery quadrupolar echo spectra (Fig. 5) in the proximity of the inversion point[1]. This further confirms that fast local exchange takes place between free water and water molecules associated via hydrogen bonds to the amide groups, which is in agreement with the findings of Mansfield et al. [8] and Loo et al. [37]. Similar results are observed for PA66 (Fig. 4(b), (e)) and annealed PA46 (Fig. 4(c), (f)).

3.5. MRI morphology of saturated PA46 plates

In order to study whether the water distribution and molecular mobility are distributed homogeneously throughout the plates, spatially resolved MRI experiments were carried out. Fig. 2(a) shows the image of a water saturated PA46 plate. Since it is acquired with an echo time (T_E) of 7 ms, only the ingressed water is visualised. Although the plate is saturated to equilibrium, the intensity of the reconstructed 1-D projection decreases gradually towards the centre of the plate. The horn shaped intensity projection is not caused by magnetic susceptibility effects since it clearly remains present upon interchanging the read (F_2) and phase (F_1) direction (figure not shown). When the ingress of water is studied as a function of time (Fig. 6), the horn shaped intensity projection appears immediately and remains present even after a period of months in water.

[1] Analyzing the T_1 of pure D_2O resulted in a single T_1 value of 400 ms. This means that the long T_1 component observed by Hutchison et al. [7] probably arises from remaining free D_2O that is trapped between the PA6 fibers and which cannot be removed by simple drying as was already suggested by Loo et al. [33]. In this study all the D_2O saturated material was shortly rinsed with water before carefully drying to exclude adsorbed D_2O.

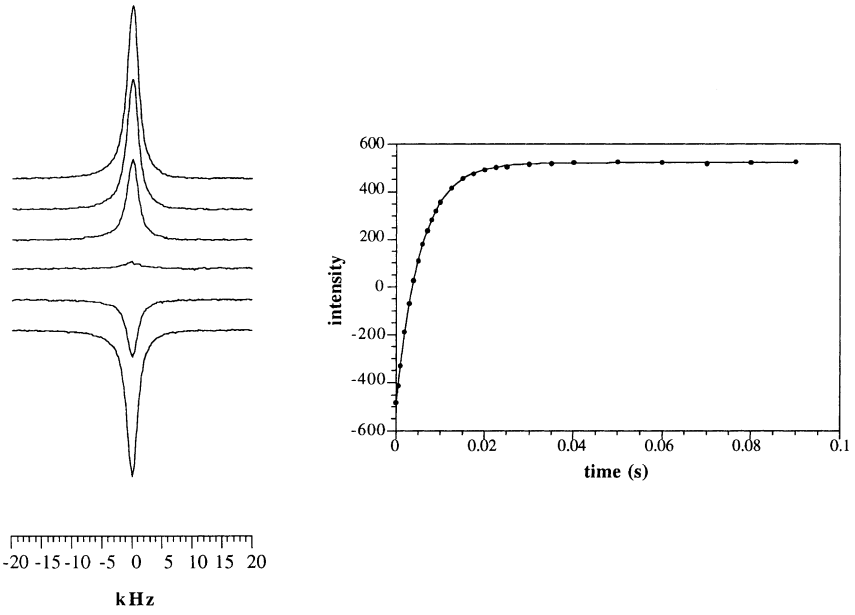

Fig. 5. Deuterium quadrupolar echo inversion recovery experiment (spectral width of 40 kHz) of D_2O saturated PA46.

Image intensity can be a rather complex function of local concentration of water (and plasticised polyamide) and of the T_1 and T_2 relaxation times, which are largely affected by molecular motions. In order to determine whether this horn shaped image intensity distribution can explain the unexpected high amount of water absorption by PA46, a more detailed spatially resolved MRI relaxation study is inevitable.

3.6. Spatially resolved MRI relaxation analysis of saturated PA46 plates

Spatially resolved MRI experiments were carried out to distinguish whether the horn shaped intensity distribution is due to concentration and/or relaxation effects. The spatially resolved values of M_0, T_1 and T_2 are presented in Table 2. While the T_1 relaxation time is almost spatially independent, the T_2 relaxation time clearly is spatially dependent. The high intensity horns at the outer layers of the plate show a biexponential T_2 decay with a slow and fast component of, respectively, 4.5 and 1.2 ms, which can be assigned to absorbed water and plasticised PA46, respectively. A gradual decrease of the T_2 value of water is observed over several tenths of a mm from the surface towards the core of the plate where a single T_2 value of 3.5 ms is observed. Analysing the intensity of the total reconstructed projection yields two T_2 decay times: T_2^s of 1.2 ms and T_2^l of 4 ms, the latter being intermediate between the value obtained in the outer layer and core part of the plate, and representing the volume averaged T_2 value of absorbed water molecules (cf. volume averaged proton T_2 measurements). The observation of a similar T_2 relaxation time for the water molecules as measured with CPMG confirms that fast local exchange takes place between free water and water molecules associated via hydrogen bonds to the amide groups. These in contrast to the large-scale molecular diffusion of water molecules, which is of course, slow (cf. spatially dependent T_2 decay).

Table 2
Spatially resolved T_1, T_2 and M_0 values of injection moulded PA46 plates saturated with water

	T_1 (s)	T_2 (ms)	M_0
Horn	0.95	4.5	4700
		1.1–1.3	1500
Core	1.17	3.5	4000
Total projection	1.07	4.0	
		1.1–1.3	

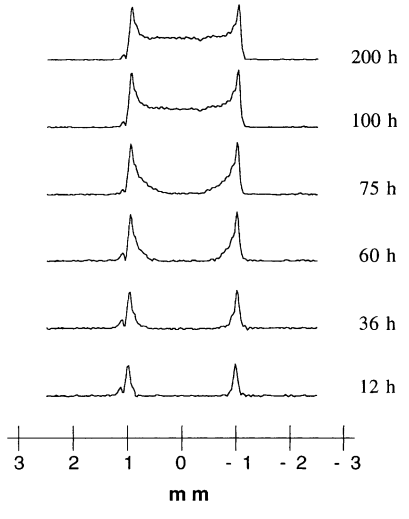

Fig. 6. 1-D reconstructed projections of MRI images ($T_E = 7$ ms, $T_R = 3.5$ s) of a 2 mm PA46 plate immersed in water at 35°C as a function of time. The surrounding water is suppressed using the IR technique.

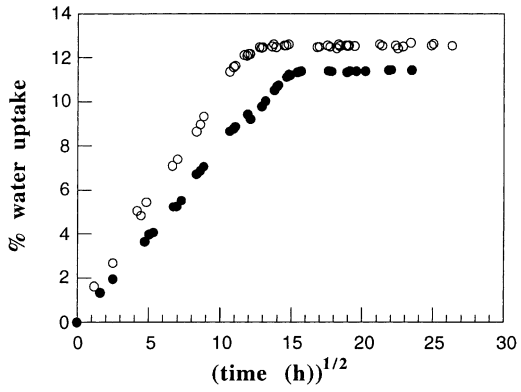

Fig. 7. Water uptake (in wt%) as a function of square root of time for (○) a native 2 mm PA46 plate and (●) a two-sided polished PA46 plate immersed in distilled water at 35°C.

As far as the spin density of water is concerned (Table 2), an excess of about 18% is observed in the horn ($M_0 = 4700$) with respect to the core part ($M_0 = 4000$). This excess of water results in a larger amount and a higher molecular mobility of the plasticised amorphous phase in the outer part of the plate and explains why the short T_2 decay time (1.2 ms) is only observed in the outer part of the PA46 plate. This plasticised amorphous phase will, however, only contribute to the intensity in images acquired with a short echo time ($T_E \ll 5$ ms). An MRI and gravimetric analysis of a two-sided polished plate indicate that the horns in an original PA46 plate largely originate from the higher amount of water in the outer layer of the plate: almost no horns appear in the image (Fig. 2(b)) and a reduced water uptake of ca. 11.4% is observed (Fig. 7). Indeed, since an original 4 mm plate absorbs 12.4% water, the outer 1 mm layer of an original plate has to absorb 13.4% water (or about 18% more than the core part) to give an average water absorption of 12.4%.

The horn shaped intensity distribution of water in images of saturated PA46 plates can be fully understood (and calculated) by these local differences in M_0 and T_2, which strongly indicate a difference in morphology between the outer layer and core part of PA46 plates.

3.7. Volume averaged proton relaxation of different parts of a dry PA46 plate

Solid echo wide-line experiments, carried out on the core material and on a 100 and a 350 μm scraped outer layer of a dry, native PA46 plate (Table 3), confirm a difference in morphology between the outer and core part of PA46 plates. At ambient temperature a single T_2 relaxation time of about 15 μs, characteristic for the crystalline and glassy amorphous phase, is obtained for all specimens. At 170°C, (almost 100°C above T_g) the solid echo decay consists of a mobile (exponential) and rigid (Gaussian) T_2 component. The fraction of the rigid component is similar to the amount of crystallinity (ca. 60–70%) as determined by WAXS (Table 1). T_1 results can be analysed monoexponentially at ambient temperature as well as at 170°C. At temperatures below T_g, a single exponential proton T_1 relaxation time is often observed in heterogeneous materials because of efficient spin-diffusion [38]. The T_1 value of the core always exceeds the T_1 value of the 100 μm scraped surface layer, while the T_1 value of the 350 μm surface layer is intermediate. These experiments confirm the difference in morphology between the outer layer and core part of PA46 plates.

3.8. Differential scanning calorimetry

Further indications of the difference in morphology between the core and outer part of PA46 plates are given by a gravimetrical analysis and DSC. Fig. 7 shows the water uptake against square root of time for an original 2 mm plate and a two-sided polished plate. Besides a lower equilibrium mass uptake, the rate of water sorption measured at 35°C for the polished plate is roughly half that of an original plate: 0.8×10^{-6} mm^2/s versus 1.5×10^{-6} mm^2/s. This explains the image in Fig. 2(c) showing the ingress of water in a one side polished plate. Only the nonpolished side shows the high intensity horn and the water ingress is slower along the polished side. Moreover the plate bends due to a larger swelling of the original side as compared to the polished side. The difference in morphology, however, is not caused by a difference in the amount of crystallinity. DSC measurements on the core part and the 100 μm scraped surface layer show no difference in the amount of crystallinity as can be concluded from an identical melting enthalpy (ca. 90 J/g) and melting temperature (ca. 290°C). Since diffusion and sorption of water only takes place in the amorphous regions and the amount of amorphous phase is constant over the total cross-section, the difference in water content and sorption rate indicates a difference in morphology of the amorphous phase. It is suggested that the mean distance between the amide groups in the amorphous phase is different in the outer and core part of the plates. This affects the strength of the hydrogen bond between the amide groups as well as the water content, which results in a gradual increase of water amount (M_0) and water molecular mobility (T_2) from the core to the outer part of the PA46 plate.

Table 3
Volume averaged solid echo proton T_1 and T_2 values at 20 and 170°C for different parts of original PA46 plates. Fractional amplitudes of relaxation components are shown between parentheses

PA46 plate	20°C	170°C	
Core	$T_1 = 2.28$ s	$T_1 = 1.52$ s	
	$T_2 = 14$ μs	$T_2 = 16$ μs	(65%)
		$T_2 = 86$ μs	(35%)
± 350 μm surface layer	$T_1 = 1.98$ s	$T_1 = 1.47$ s	
	$T_2 = 17$ μs	$T_2 = 15$ μs	(63%)
		$T_2 = 67$ μs	(37%)
100 μm surface layer	$T_1 = 1.80$ s	$T_1 = 1.24$ s	
	$T_2 = 14$ μs	$T_2 = 13$ μs	(62%)
		$T_2 = 50$ μs	(38%)

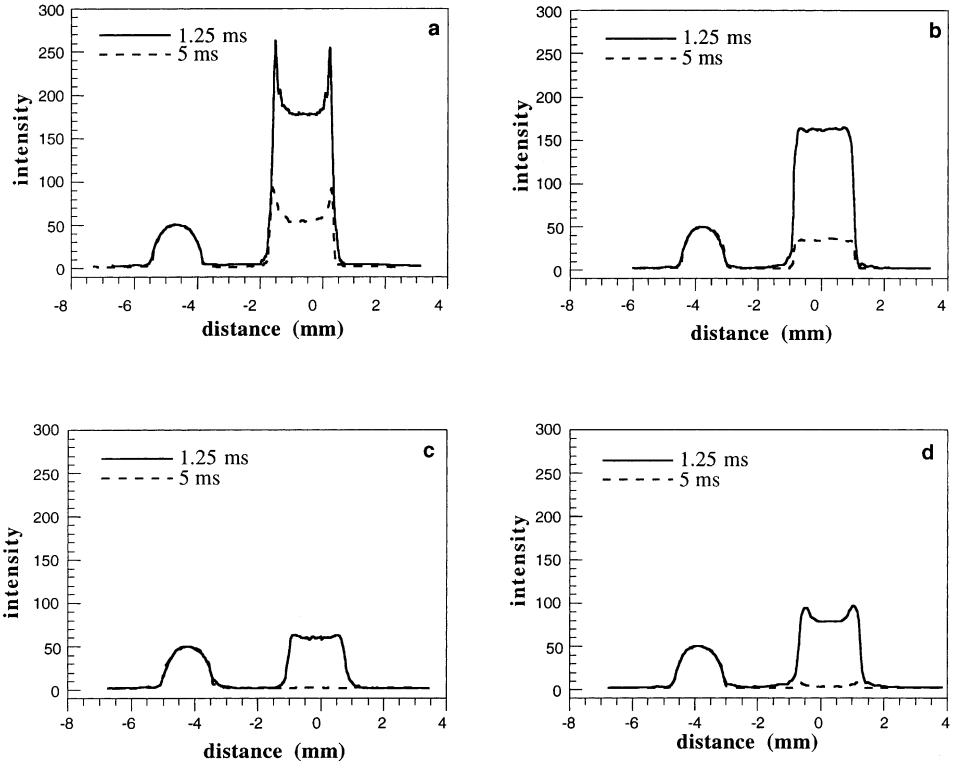

Fig. 8. 1-D reconstructed projections of MRI images (— : $T_E = 1.25$ ms, –-: $T_E = 5$ ms) of (a) an original 2 mm PA46 plate; (b) a two-sided polished PA46 plate; (c) an annealed PA46 plate and (d) an original PA66 plate, all after immersion in water for one month. Images are recorded without surrounding water and in the presence of a reference capillary filled with doped water (left side of the projection). Remark that for $T_E = 1.25$ ms the intensity of the horns in Fig. 8(a) is higher than its value calculated from the water content and T_2 relaxation time, since with this short echo time also a fraction of the plasticised nylon is observed.

3.9. Intensity calibrated MRI images

Fig. 8 shows the reconstructed projections of images ($T_E = 1.25$ ms and $T_E = 5$ ms) of an original, a polished and an annealed PA46 plate and a PA66 plate, all saturated with water to equilibrium. The volume averaged T_1 and T_2 relaxation times are presented in Table 4. By means of the water uptake and the (local) T_2 values presented in Tables 2 and 4, the intensities of all 1-D projections shown in Fig. 8 can be fully explained by means of Eq. (3). As mentioned before, the two-sided polished plate shows no high intensity horns. Although an annealed PA46 plate contains 6.2% water and the amount of crystallinity increases only slightly (70%) [1] upon annealing, no intensity is observed in images recorded with $T_E = 5$ ms (Fig. 8(c)). Signal intensity is only detected with a shorter $T_E = 1.25$ ms. Although fast local exchange of water molecules still takes place after annealing (Fig. 4), the average T_2 relaxation time of water decreases to such an extent that no signal is observed at $T_E = 5$ ms. This confirms that the chain arrangement in the amorphous phase rather than the amount of amorphous phase determines the observed signal intensity since it affects the average molecular mobility and amount of absorbed water. Also in saturated PA66 plates, containing 8.5% water and having a crystallinity of 50%, almost no signal intensity is observed in images recorded with $T_E =$ 5 ms (Fig. 8(d)). Images acquired with $T_E = 1.25$ ms also tend to show a horn shaped intensity distribution, but the intensity of the horns is much smaller as compared to PA46 plates.

Table 4
Water content and volume averaged T_1 and T_2 relaxation times for different polyamides saturated with water

	Water uptake (wt%) at equilibrium	T_1 relaxation time (s)	T_2 relaxation time (ms)
Original PA46	12.4	1.07	4.0 1.1–1.3
Two-sided polished PA46	11.4	1.28	2.8
Annealed PA46	6.2	2.22	1.4
PA66	8.5	1.36	1.4

The following model is proposed to explain the origin of the higher water absorption and water mobility in PA46 as compared to PA6 and PA66. The very high crystallisation rate of PA46 (Table 1), together with the fast cooling rate from the melt to the temperature in the mould, prevents a mutual chain arrangement in the amorphous phase, i.e. a close coupling of amide groups in the amorphous phase. This results in a gradual decrease of the amorphous density from the core towards the outer parts of the plates. This

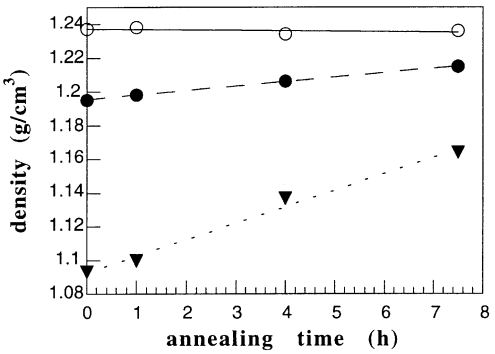

Fig. 9. Density of (▼) the amorphous phase ρ_a, (○) the crystalline phase ρ_c, and (●) the overall density ρ (in g/cm^3) of PA46 plates as a function of the annealing time.

difference in amorphous density is especially observed at the outer part of the plate due to the faster cooling of the outside in the mould. It is suggested that the average distance between the amide groups in PA46 is somewhat larger, resulting in an increased water absorption and a higher mobility (T_2) of the water molecules. The concept of the relation between water absorption and density of the amorphous phase in PA46 is confirmed by WAXS and density measurements. Fig. 9 shows the density of the crystalline phase ρ_c (determined by WAXS), and the overall density ρ (determined via gradient column) for PA46 as a function of annealing time. The density of the amorphous phase (ρ_a), which can be calculated from the overall density, the crystalline density and an average crystallinity of 71% of PA46, increases significantly as a function of the annealing time. The amount of crystallinity and the density of the crystalline phase on the other hand, remain almost constant upon annealing.

This concept furthermore explains the water uptake after annealing. Annealing of PA46 results in a water absorption and mobility of water molecules similar to that in PA6 and PA66 (Fig. 8(c) and (d)). During annealing at 260°C, the density of the amorphous phase of PA46 increases, resulting in a substantial decrease of water uptake and molecular mobility of water molecules. Because of the higher crystallinity of annealed PA46, the total water uptake is substantially lower than for PA66 (Table 5). When related to the amorphous phase, however, the water uptake of PA66 and annealed PA46 are almost equivalent.

4. Conclusions

MRI and volume averaged ^{1}H and ^{2}H NMR relaxation experiments have been performed to study the difference in water absorption in injection moulded plates of PA46, PA6 and PA66. The higher amount and higher molecular mobility of water molecules in the PA46 plates can be explained by the substantially higher crystallisation rate of PA46 compared to the other polyamides. The higher crystallisation rate hampers the close coupling of amide groups in the amorphous phase, which results in a larger mean distance between the amide groups in the amorphous phase of PA46. PA46 therefore absorbs a substantially higher amount of water and the absorbed water molecules have a higher molecular mobility (T_2) compared to PA6 and PA66. These differences are noticeably larger in the outer part of the PA46 plates due to the faster cooling of this part to the temperature of the mould, which is significantly lower than the crystallisation temperature. Annealing of PA46 causes an increase of the amorphous density (confirmed by WAXS and gradient column), resulting in a strongly reduced water molecular mobility and a water absorption similar to PA6 and PA66. In comparison with PA6 and PA66, annealed PA46 shows an almost equivalent water uptake when related to the amorphous phase, but the total water uptake is significantly lower because of the higher crystallinity.

Table 5
Water absorption by original PA46, annealed PA46 and original PA66 injection moulded plates

	Water uptake (wt%) at equilibrium	% amorphous phase	Water content in the amorphous phase (%)
PA46	12.4	30	41
Annealed PA46	6.2	30	20
PA66	8.5	50	17

Acknowledgements

We wish to thank Dr H. van Well and Dr M. Klinkenberg for their participation in an early phase of this work, G. Reggers for providing the DSC runs and J. Kaelen for technical support.

References

[1] Eltink S, de Boer S, Moonen J. Crystallinity studies on polyamides, Internal publication. The Netherlands. DSM Research, 1992.
[2] Kawasaki K, Sekita Y. J Polym Sci: Part A 1964;2:2437.
[3] Razumovskii LP, Markin VS, Zaikov GY. Polym Sci USSR 1985;27:751.
[4] Fukuda M, Miyagawa M. Hyogo Kyoiku Daigaku Kenkyu Kiyo, Dai-3-bunsatsu 1995;15:125.
[5] Murthy NS, Stamm M, Sibilia JP, Krimm S. Macromolecules 1989;22:1261.
[6] Knopp B, Suter UW. Macromolecules 1997;30:6114.
[7] Hutchison JL, Murthy NS, Samulski ET. Macromolecules 1996;29:5551.
[8] Mansfield P, Bowtell R, Blackband SJ. Magn Reson 1992;99:507.
[9] Murthy NS, Akkapeddi MK, Orts WJ. Macromolecules 1998;31:142.
[10] Murthy NS, Orts WJ. J Polym Sci B: Polym Phys 1994;32:2695.
[11] Plestil J, Baldrian J, Ostanevich YM, Bezzabotnov VY. J Polym Sci B: Polym Phys 1991;29:509.

[12] Fyfe CA, Randall LH, Burlinson NE. J Polym Sci A: Polym Chem 1993;31:159.
[13] Aminabhavi TM, Phayde HTS. Polymer 1995;36:1023.
[14] Crank J, Park GS. Diffusion in polymers. New York: Academic Press, 1968.
[15] Lauterbur P. Nature 1973;242:190.
[16] Ercken M, Adriaensens P, Vanderzande D, Gelan J. Macromolecules 1995;28:8541.
[17] Weisenberger LA, Koenig JL. Macromolecules 1990;23:2445.
[18] Blackband S, Mansfield PJ. Phys C Solid State Phys 1986;19:L49.
[19] Weisenberger LA, Koenig JL. Appl Spectrosc 1989;42:1117.
[20] Lauenstein A, Tegenfeldt J, Kuhn W. Macromolecules 1998;31:3886.
[21] Blümich B, Kuhn W. Magnetic resonance microscopy. New York: VCH Weinheim, 1992.
[22] Hyde TM, Gladden LF, Mackley MR, Gao P. J Polym Sci A Polym Chem 1995;33:1795.
[23] Hyde TM, Gladden LF. Polymer 1998;39:811.
[24] Mansfield P, Bowtell RW, Blackband SJ, Cawely M. Magn Reson Imaging 1991;9:763.
[25] Webb AG, Hall LD. Polymer 1991;32:2926.
[26] De Crespigny AJS, Carpenter TA, Hall LD, Webb AG. Polym Commun 1991;32:36.
[27] Crank J. The mathematics of diffusion. 2nd ed. London: Oxford University Press, 1975.
[28] Rezac ME, John T. Polymer 1998;39:599.
[29] Chin JW, Nguyen T, Aouadi K. J Appl Polym Sci 1999;71:483.
[30] Liu J, Nieminen AOK, Koenig JL. J Magn Reson 1989;85:95.
[31] Meiboom S, Gill D. Rev Sci Instrum 1958;29:688.
[32] Powles JG, Stange JH. Proc Phys Soc 1963;82:6.
[33] Fedotov D, Schneider H. Structure and dynamics of bulk polymers by NMR-methods. Berlin: Springer, 1989.
[34] Vold RL, Waugh JS, Klein MP, Phelps DEJ. Chem Phys 1968;48:383.
[35] Hirschinger J, Miura H, Gardner KH, English AD. Macromolecules 1990;23:2153.
[36] Miura H, Hirschinger J, English AD. Macromolecules 1990;23:2169.
[37] Loo LS, Cohen RE, Gleason KK. Macromolecules 1998;31:8907.
[38] Douglas DC, Jones GP. J Chem Phys 1966;45:956.